2017 International Nuclear Atlantic Conference - INAC 2017
Belo Horizonte, MG, Brazil, October 22-27, 2017
ASSOCIAÇÃO BRASILEIRA DE ENERGIA NUCLEAR – ABEN

Agência Brasileira do ISBN
ISBN 978-85-99141-07-6
9 788599 141076

A THIRD GENERATION TOMOGRAPHY SYSTEM WITH FIFTEEN DETECTORS AND A GAMMA-RAY SOURCE IN FAN BEAM GEOMETRY SIMULATED BY MONTE CARLO METHOD

A.F. Velo; A. G. Alvarez, D.V.S. Carvalho; V. Fernandez, S. Somessari, F. F. Sprenger, M.M. Hamada and C.H. Mesquita

Instituto de Pesquisas Energéticas e Nucleares (IPEN / CNEN - SP)
Av. Professor Lineu Prestes 2242
05508-000 São Paulo, SP
chmesqui@usp.br

ABSTRACT

This paper describes the Monte Carlo simulation, using MCNP4C, of a multichannel third generation tomography system containing a two radioactive sources, ^{192}I (316.5 – 468 KeV) and ^{137}Cs (662 KeV), and a set of fifteen NaI(Tl) detectors, with dimensions of 1 inch diameter and 2 inches thick, in fan beam geometry, positioned diametrically opposite. Each detector moves 10 steps of 0,24°, totalizing 150 virtual detectors per projection, and then the system rotate 2 degrees. The Monte Carlo simulation was performed to evaluate the viability of this configuration. For this, a multiphase phantom containing polymethyl methacralate (PMMA (($\rho \cong$ 1.19 g/cm^3)), iron ($\rho \cong$7.874 g/cm^3), aluminum ($\rho \cong$ 2.6989 g/cm^3) and air ($\rho \cong$ 1.20479E-03 g/cm^3) was simulated. The simulated number of histories was 1.1E+09 per projection and the tally used were the F8, which gives the pulse height of each detector. The data obtained by the simulation was used to reconstruct the simulated phantom using the statistical iterative Maximum Likelihood Estimation Method Technique (ML-EM) algorithm. Each detector provides a gamma spectrum of the sources, and a pulse height analyzer (PHA) of 10% on the 316.5 KeV and 662 KeV photopeaks was performed. This technique provides two reconstructed images of the simulated phantom. The reconstructed images provided high spatial resolution, and it is supposed that the temporal resolution (spending time for one complete revolution) is about 2.5 hours.

1. INTRODUCTION

Multiphase systems are structures that contain a mixture of solids, liquids and gases inside a chemical reactor or pipes in a dynamic process. These systems are widely used by the chemical, food, pharmaceutical and petrochemical industries. The gamma ray CT system has been applied to visualize the distribution of multiphase systems, providing analysts and engineers the means to obtain measurements in real time without actually interrupting production. CT systems have been used to improve design, operation and troubleshooting of industrial processes. Computer tomography for multiphase processes is now a promising technique being developed at several advanced research laboratories [1, 2].

Scanners for transmission tomography employ radioisotope sources positioned on one side of the object to be scanned and one, or a set of, collimated detectors arranged on the opposite side [3]. Currently, scanners typified as third and fourth generations are commonly used in industrial applications. Usually, the third generation CT systems have better spatial resolution, while fourth-generation CT systems have enhanced temporal resolution (time

needed to obtain an image). Also it is capable of generating images at a faster rate but generally with lower spatial resolution. On the other hand, if spatial resolution is important and knowledge of dynamic phenomena can be limited to their trends, then third generation CT systems should be a suitable choice [4, 5].

Usually, the analyzed objects in the industrial tomography field, such as distillation columns and engines, contain materials with a large range of densities, for example iron (7.8 g/cm^3), aluminum (2.7 g/cm^3), water (1.0 g/cm^3), gases (0.000125 g/cm^3) [6]. Thus, ideally, radioactive sources containing different gamma energies should be used [7]. The combination of ^{137}Cs with ^{192}Ir or ^{137}Cs with ^{75}Se could be used as their energy spectra present energy peaks of 662, 468, and 317 keV for a ^{137}Cs + ^{192}Ir combination or 662, ≅132, ≅269 and 401 keV for a ^{137}Cs + ^{75}Se combination [8]. Moreover, in case the object to be analyzed contains high-density material, the ^{60}Co (1173 and 1332 keV [8]) can be included in the source combination to allow the beam to cross the materials. However, depending on the density and dimension of the object the ^{241}Am (59 keV [8]) can be added to the source combination in order to improve the image quality in the regions where low density material is present. Moreover, if the image details of the object edge are important for the analysis, thus photons with low energy are preferable because the path of radiation absorption in the object edge is relatively small.

CT systems measure linear attenuation coefficients, μ(cm-1) which depends on material density. Generically, high-density material implies a reduction of the transmitted beam. According to the attenuation exponential law (Beer-Lambert's law), the fraction of a beam from high-energy radiation that crosses an object of high density is higher when compared to that low-energy radiation. This effect is caused by the decrease of the mass coefficient μ (cm-1) as the energy of the radiation increases. Thus, for objects containing different density materials, ideally, the tomographic measurement should be carried out, using different energies from gamma rays. In this case, the CT data acquisition system should have the ability to discriminate between different gamma ray energies. An arrangement with ^{192}Ir (≅317 and ≅468 keV), ^{137}Cs (662 keV) and ^{60}Co (1173 and 1332 keV) sources meets this need. Alternatively, depending on the density profile of the multiphase components, a single radioisotope source, such as ^{75}Se (≅132, ≅269 and 401 keV), could be used [7].

Some laboratories use two radioactive sources with two sets of detectors and single channel counters, spaced at 90 degrees [7, 9]. However, this option has the inconvenience of needing a double set of detectors and counters. Instead, fast multichannel counters with a single set of detectors can be used. This alternative meets the requirements of the CT system for multiphase system analysis more efficiently since the number of shielded sources, detectors and counters are reduced.

In this study, a third generation multi-source transmission computed tomography system with a multichannel data acquisition electronic system was simulated. Two different radioactive sources, ^{192}Ir and ^{137}Cs placed in a single lead collimation system and fifteen NaI(Tl) detectors of 1 inch diameter and 2 inches thick comprise this tomography. The capacity of this CT system to determine and differentiate the attenuation coefficients of materials with different phases (gas, liquid, solid) was studied using different radioisotope energies and a phantom comprised a polymethylmethacrylate (PMMA) solid cylinder containing three holes: one filled with a steel plug, another with an aluminum plug and the third one empty (filled with air) and surrounded with glass.

2. MATERIAL AND METHODS

2.1.Monte Carlo Simulation.

A third multichannel industrial generation computed tomography system, comprising fifteen NaI(Tl) detectors of ø1 x 2 inches (diameter, thickness) was simulated. The detectors were placed on a gantry in fan-beam geometry opposite to the gamma ray source, as shown in Fig.1. The fifteen NaI(Tl) detectors were individually collimated with lead containing a septa of ø 0.196 x 1.96 inches (diameter, depth). The detectors move 10 times in a step angle of 0.23 degree, emulating 150 detectors per projection. Thereafter, the support table containing the gantry and the ^{137}Cs gamma source (Fig. 1) rotates 2 degrees forward, and this process goes on up to completing 360 degrees, totalizing 180 projections. For a total of 2700 samples (150 'virtual detectors' x 180 projections) the system is supposed to spend 9000 seconds or 2.5 hours to obtain each tomography image. The ^{192}I and ^{137}Cs radioactive sources, of ≅317, ≅ 468 KeV and 662 KeV of energy respectively, were placed into a radioactive shield-case with an aperture angle of 36 degrees. This system was previously described by Mesquita et al [12,13].

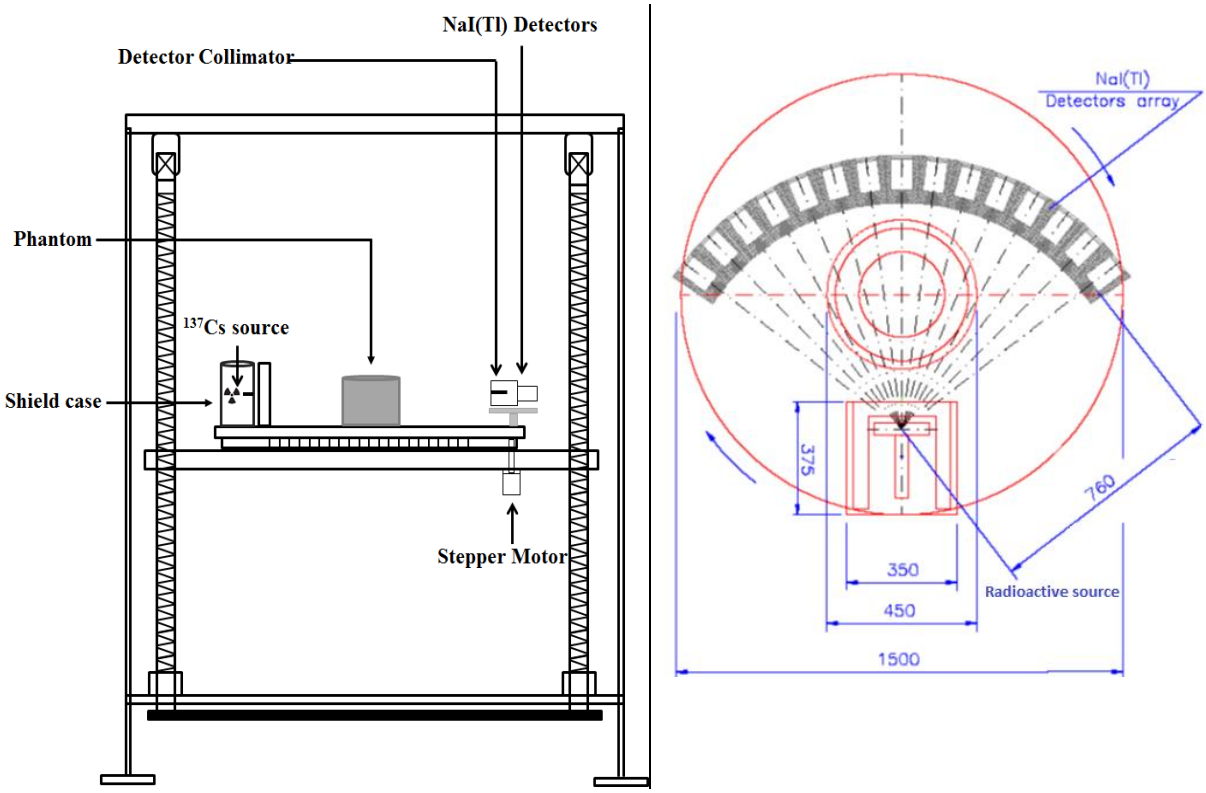

(a) (b)

Figure 1: Diagram of the third generation CT scanner used. (a) Side view and Top view (b)

When performing the mathematical simulation of NaI(Tl) detectors, in order to obtain their response curves, some corrections should be made to improve the simulation approaching to the real case. Two of the main corrections are essentials: the determination of the photon detection efficiency and the resolution energy, which is related to distinguish different peaks

very close to each other in the energy spectrum [10-12]. In practice, the energy resolution of the detector is given by the full width at half maximum (FWHM) of the Gaussian peak (pulses per channel) for a given energy [10, 12, 13].

Some of the effects related to the photopeak are inherent to the electronic circuit of the spectrometric system which is not simulated by the MCNP. Thus, to optimize the detector response and consider these physical effects in the simulation, it is necessary to obtain experimentally adjustment parameters of the detector energy resolution and apply a MCNP code function to fits the Gaussian to the spectrum obtaining the proper corrections [10].

The MCNP fitting technique to take into account the resolution of the real detector, measured experimentally, consists of using a "FT8 GEB" card into the input file of the code. The tallied energy is broadened by sampling from Gaussian [10,12].

A non-linear function adjusted by least-squares procedure was used as an input to the MCNP code, using a fitting function [14]. These parameters should be used with the Gaussian Energy Broadening (GEB) command in order to consider the energy resolution of the detector in the simulation [10, 12]. GEB is a special treatment for tallies to better simulate a physical radiation detector in which energy peaks exhibit Gaussian energy broadening. This parameters was calculated in previous works [12].

For the estimation of the pulse height, a F8 tally was applied on MCNP code to obtain the deposited energy distribution per incident photon on the NaI(Tl) detector, where for each individual history, the tally accumulates the deposited energy. In order to obtain a good statistic counts, the histories number used was 11E+09.

2.1. Multiphase Phantom and CT Characterization

A multiphase phantom was simulated to evaluate the performance of the multichannel third generation industrial tomography system device. The phantom consists of a PMMA ($\rho \approx 1.19$ g/cm3 [6]) solid cylinder containing three holes: one filled with steel ($\rho \approx 7.874$ g/cm^3[6]), another with aluminum ($\rho \approx 2.698$ g/cm^3[6]) and the third one empty (filled with air) and surrounded with glass, as illustrated in Fig. 3.

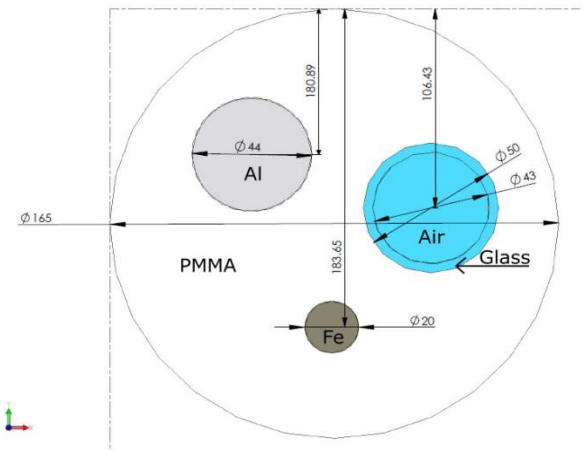

(A) (B)

Figure 3: Picture (A) and Illustration of the multiphase phantom scheme. 1- Air surrounded with glass wall, 2-aluminum bar and 3-steel bars. The phantom is made of acrylic (B)

2.3. Iterative Algorithms

The image reconstruction is based on the exponential decay law defined by the equation (1), which is known as Lambert-Beer's law [15]:

$$I=I_0 \cdot e^{\sum_{i=1}^{N} \mu_i \cdot w_{i,\vec{j}}} \quad (1)$$

Where, I_0 is the initial intensity of the beam radiation that focuses on the object on $\vec{j}$ direction, I is the intensity of the beam radiation through the object, N is the number of pixels on matrix, $\boldsymbol{\mu_I}$ is the mass attenuation coefficient of the matter on pixel $\boldsymbol{I}$ and $w_{i,\vec{j}}$ is the length of the beam radiation through the pixel on pixel $\boldsymbol{I}$ on$\vec{j}$. $w_{i,\vec{j}}$ is defined as weighted matrix (W) (Fig. 3) element [15].

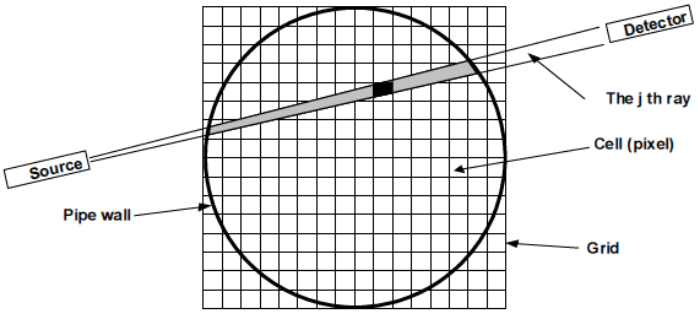

Figure 3: Discretized object [15].

The discretized ray sum for each ray j (j = 1, 2, …, J) can be expressed as the equation (2) [15].

$$p_j^{normalized} = ln\left(\frac{I_{oj}}{I_j}\right) = \sum_{i=1}^{N} w_{ij}\mu_i \quad (2)$$

Where, N is the number of pixels. The term w_{ji} represents an element of the weight matrix (W), and is defined as the intersectional area between the j^{th} ray and the i^{th} pixel divided by the intersectional area between the j^{th} ray and the sample. The size of W is defined by the number of pixels in the reconstruction grid. Due to Poisson noise corruption of the measured data, a term $\eta_j$describing the noise is added to the equation (3) [15]:

$$p_j^{normalized} = ln\left(\frac{I_{oj}}{I_j}\right) = \sum_{i=1}^{N} w_{ij}x_i + \eta_j \quad (3)$$

Solving a high number of linear equations based on measurements corrupted by random variables and noise, requires the use of iterative algorithms. The iterative methods are divided in two categories, the algebraic and the statistical [15]. Algebraic reconstruction methods solve a set of linear equations by comparing the measured data set to an estimate and reduce the difference between these. Statistical methods reconstruct the image by implementing the maximization of the likelihood function, recognizing the Poisson distribution function of the projections with the measured [15]. In the present work, the Simultaneous Iterative Reconstruction Technique (SIRT), Maximum Likelihood Expectation Maximization (MLEM) was used to reconstruct the images.

The statistical method MLEM is expressed by equation (4) respectively [3, 15].

$$f_j^{(n+1)} = \frac{\sum_{i=1}^{M}\left[I_0 e^{\left(-\sum_{k=1}^{N} h_{ik} f_k^{(n)}\right)}\left(1 - e^{-h_{ij} f_j^{(n)}}\right)\right]}{\sum_{i=1}^{M}\left[I_i - \overline{I_i} + 0.5(1 + e^{-h_{ij} f_j^{(n)}}) I_0 e^{\left(-\sum_{k=1}^{N} h_{ik} f_k^{(n)}\right)}\right]} \qquad (4)$$

All reconstruction was performed in a matrix of 128 x128 pixels and 100 iterations and performed by the Matlab 2013b®.

For the reconstruction it was considered only the energy peaks of 317 KeV of the ^{192}Ir and 662 KeV of the ^{137}Cs. For this, for each revolution, it is possible to obtain two images.

3. RESULTS AND DISCUSSION

The multichannel spectrum of ^{192}Ir and ^{137}Cs obtained by the simulated NaI(Tl) detectors is shown by Fig. 4. From this figure, it is possible to observe the different peaks corresponding the energies from respective sources. The reconstructed images of the simulated phantom were performed by these peaks.

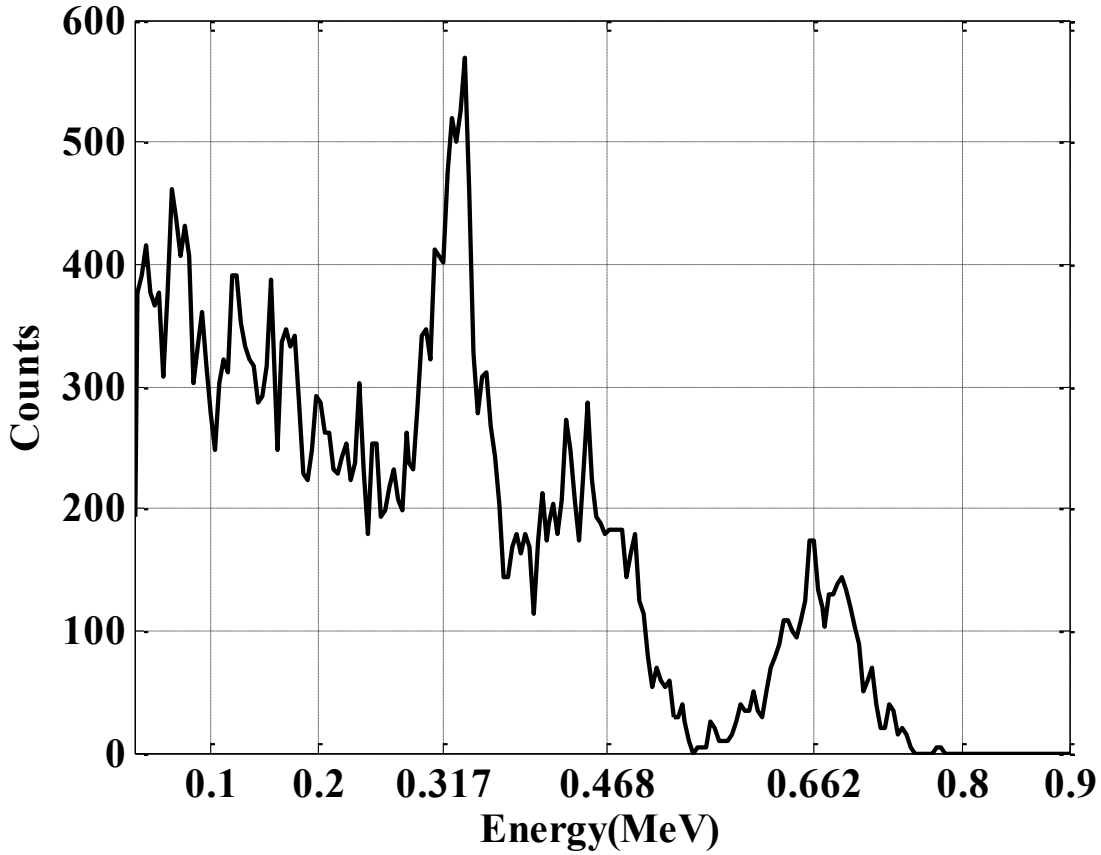

Figure 4: Simulated multichannel spectrum

The reconstructed images of the simulated phantom (Fig. 3) obtained by the simulation of the third generation tomography system, are presented in Fig. 5, where Fig. 5(a) and 5(b) presents the sinogram of the simulated phantom using the 317 KeV ^{192}Ir and 662 KeV ^{137}Cs respectively. Fig. 5(c) and 5(d) presents the reconstructed images using the 317 KeV ^{192}Ir and ^{137}Cs 662 KeV respectively.

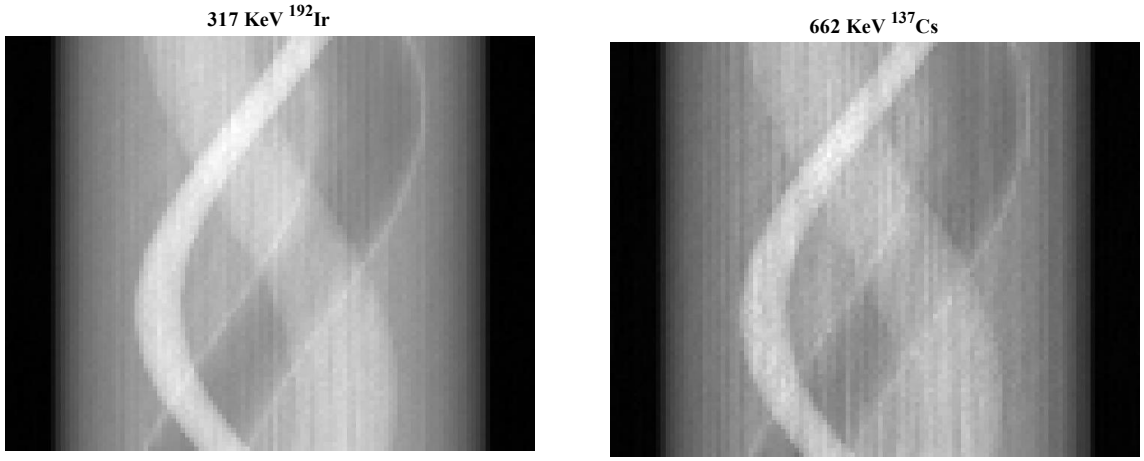

(A) (B)

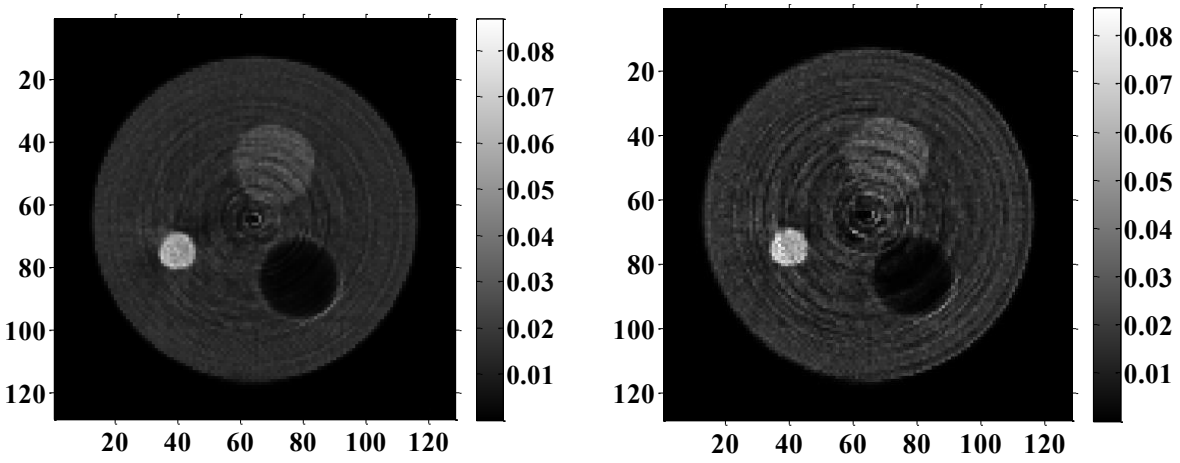

Figure 5: (a) and (b) Sinogram of the simulated phantom with 317 KeV and 662 KeV, (c) and (d) reconstructed images using 317 KeV and 662 KeV.

From the reconstructed images presented in Fig. 5, it is possible to infer that the proposed con figuration of the third generation tomography system is feasible, since these images presented good spatial resolution with a reasonable temporal resolution, besides the advantage of the multichannel, which is possible to obtain more than one image per revolution.

CONCLUSION

The simulation of the proposed tomography showed that the system has suitable capacity to distinguish several structures in the multiphase systems. Simulated results demonstrated the feasibility of the development of the third generation tomography containing fifteen NaI(Tl) detectors and boards of multichannel acquisition system. A high spatial resolution was observed in the reconstructed images, a temporal resolution about 2.5 hours is estimated.

ACKNOWLEDGMENTS

The authors would like to express their gratitude to CNPq (The Brazilian National Research Council) and FAPESP (Foundation for Research Support of the State of São Paulo) for financial support and fellowships.

REFERENCES

1. JOHANSEN G.A, HAMPEL U., HJERTAKER B. T, Flow imaging by high speed transmission tomography. *Applied Radiation and Isotopes*, **vol. 68**, nº 4-5, p. 518–524(2010)
2. FALAHI F. Al., Al-DAHHAN M., Experimental investigation of the pebble bed structure by using gamma ray tomography, *Nuclear Engineering and Design*, **vol 310**, pp.- 231-246(**2016)**
3. IAEA-TECDOC-1589, , *Industrial Process Gamma Tomography*., International Atomic Energy Agency, Vienna (2008).

4. MESQUITA C.H., VASQUEZ P.A.S., CALVO W.A.P., CARVALHO D.V.S., MARCATO L.A., MARTINS J.F.T., HAMADA M.M., Multi-source third generation computed tomography for industrial multiphase flows applications. in Conf. Rec. 2011 IEEE Nuclear Science Symposium, New York, p. 1294-1302 (2011).
5. MESQUITA C.H., DANTAS C.C., COSTA F.E., CARVALHO D.V.S., MADI FILHO T., VASQUEZ P.A.S., HAMADA M.M., Development of a Fourth Generation Industrial Tomography for Multiphase Systems Analysis, in Conf. Rec. 2010 IEEE Nuclear Science Symposium, New York, p. 19-23(2010).
6. Disponível em <https://physics.nist.gov/cgi-bin/Star/compos.pl?matno=104>, acesso em 30 set 2017.
7. DE MESQUITA, C.H. ; VELO, A.F. ; CARVALHO, D.V.S. ; MARTINS, J.F.T. ; HAMADA, M.M. . Industrial tomography using three different gamma rays. *Flow Measurement and Instrumentation*, **v. 47**, p. 1-9 (2016).
8. Disponível em <https://www.inl.gov/>. Acesso em 30 set 2017.
9. BENAC J., Alternating minimization algorithms for X-ray computed tomography: multigrid acceleration and dual energy application, Tese (Ph.D), Washington University, St. Louis, 2005.
10. SALGADO, C.M., BRANDÃO L.E.B., SCHIRRU, R., PEREIRA, C.M.N.A.. CONTI C.C. Validation of a NaI(Tl) detector's model developed with MCNP-X code. *Progress in Nuclear Energy*, v. 59, p. 19-25 (2012).
11. JEHOUANI, A., ICHAOUI, R., BOULKNEIR, M. Study of the NaI(Tl) efficiency by Monte-Carlo method. *Applied Radiation and Isotopes*, **v. 53** (4-5), p. 887-891 (2000)
12. VELO A.F, HAMADA M.M., CARVALHO D.V.S., MARTINS J.F.T, MESQUITA C.H., A portable tomography system with seventy detectors and five gamma-ray sources in fan beam geometry simulated by Monte Carlo method. *Flow Meas. Instr*, v. 53, p. 89-94 (2017).
13. HADIZADEH YAZDI M.H., MOWLAVI A.A., THOMPSON M.N., MIRI HAKIMABAD H. Proper shielding for Na(Tl) detectors in combined neutron-gamma fields using MCNP. *Nuclear Instruments and Methods in Physics*,.**v. 522**, p. 447-454(2004)
14. PELOWITZ, D.B. MCNP-X TM *User's Manual*, Version 2.5.0, LA-CP-05-0369. Los Alamos National Laboratory (2005).
15. MAAD R., HJERTAKER B.T., JOHANSEN G.A, OLSEN Ø. Dynamic characterization of a high speed gamma-ray tomography. *Flow Measurement and Instrumentation*, **v. 21**, p. 538-545(2010).